Accepted Manuscript

Geological Society, London, Special Publications

Characteristics of a wing-like sandstone intrusion, Volund Field

Nicholas Satur, Andrew Hurst, Asgeir Bang, Ivar Skærpe & Sarah Alexandra Muehlboeck

DOI: https://doi.org/10.1144/SP493-2017-309

Received 19 November 2017
Revised 18 January 2020
Accepted 13 February 2020

Characteristics of a wing-like sandstone intrusion, Volund Field.

Nicholas Satur*, Andrew Hurst#, Asgeir Bang, Ivar Skjærpe and Sarah Alexandra Muehlboeck

Aker BP ASA, Jåttåvågveien 10, Hinna Park, 4020 Stavanger, Norway.

#Department of Geology and Petroleum Geology, University Aberdeen, King's College, Aberdeen AB24 3UE, UK

*Correspondence (nicholas.satur@akerbp.com)

Abstract: Reservoirs in the Volund Field are all sandstone intrusions with wings on three sides forming the main reservoir volumes. The southern wing was the target of exploration and appraisal wells, which led to the field development. Identification of three smaller intrusions prove the southern wing is a composite intrusion, similar to outcrop analogues. Identification from core and borehole logs shows it comprises sandstone, mudstone and mudstone-rich intervals, including mudstone clast breccia. Mudstone clast breccia constitutes a significant missed pay candidate. Breccia is porous and has a sand-supported matrix, which gives it excellent reservoir quality. This may be missed pay using analysis of borehole logs. Well data, largely borehole logs, show consistently uniform sandstone porosity distribution within the intrusions, independent of depth. Significantly, at about 100m from the depth at which the wing emanates from sills, porosity has a broader spread of values. The spread of values is attributable to mudstone clast breccia and thin-bedded sandstone and mudstone. Porosity derived from borehole logs does not differentiate breccia from siltstone, but inference is possible using calibration of logs with core.

Introduction

Sandstone intrusions with wing-like and saucer-shaped geometry are typical targets of exploration and field development wells in sand injection complexes (MacLeod *et al.* 1999; Duranti *et al.* 2002; Huuse *et al.* 2003; Hurst *et al.* 2005; DeBoer *et al.* 2007; Szarawarska *et al.* 2010). Outcrop observations of discrete wing-like intrusions (Huuse *et al.* 2007; Zvirtes *et al. this volume*) and wings as parts of composite saucer-shaped intrusions (Vigorito & Hurst 2010, Hurst & Vigorito 2017; Grippa *et al.* 2019) are similar to subsurface intrusions. Seismic mapping reveals the Volund Field is consists of wings on three sides to the north, east and south (Fig.1). Much of the detail visible at outcrop (e.g. Zvirtes *et al. this volume*) is unresolved on seismic data and if Volund's southern wing, the focus of this paper, is a discrete sandstone intrusion it is exceptionally large when compared to outcrop analogues.

The Volund Field is a successful development of an injected sandstone reservoir, located in the Norwegian North Sea and set in production in 2009 (DeBoer *et al.* 2007, Townsley *et al.* 2012). However, the discovery was initially discounted when two exploration wells 24/9-5 and -6 were drilled in 1993-4 and were interpreted as depositional turbidite sandstones with little economic reserves. Later models of injection wings led to new play definition and new drive to drill further exploration/appraisal wells to prove the injection model with sufficient reserves to develop resulting in first oil in 2010. The numerous near vertical and horizontal wells that penetrated the southern wing of the Volund Field, and good quality of the seismic data, allow for investigation of the characteristics of the southern wing. Volund's exploration and appraisal wells proved the presence of sandstone intrusion reservoirs by linking core facies with seismic geomorphology (DeBoer *et al.* 2007). Drilling

of three additional laterals explored the down- and up-flank variability in thickness, facies, reservoir quality, and tied to the seismic data (Figs. 1, 2; Townsley *et al.* 2012; Schwab *et al.* 2014). In light of the new data, the re-examination of core from two earlier exploration wells (24/9-5 and 24/9-6), which originally assigned a depositional origin, were re-assigned an injected origin, and interpreted as close to bedding parallel sills (Fig. 2).

Where cores were available, identification of high-quality reservoir sandstone was common however, poorer quality mudstone-rich units were also present, including mudstone clast breccia (DeBoer *et al.* 2007). By referencing outcrop analogue data, it seemed likely that some mudstone was interbedded with intrusions, or mudstone units were disrupted during hydraulic fracturing and sand injection (Schwab *et al.* 2014; Hurst *et al.* 2016). With this in mind, searching for evidence of possible composite intrusions was a priority during seismic interpretation and combined with careful analysis of borehole logs, the results of this work are the subject of this paper. Identification of these composite intrusions has led to drilling of additional production wells in 2016-7 targeting poorly drained or undrained oil, increasing the oil reserves of the field.

Geological background

Volund, and associated satellite fields Viper and Kobra (Fig. 1a), are part of a larger sand injection complex that were emplaced into the Balder Formation (lowest Eocene age) during the early Eocene. Precise timing is unknown as criteria such as associated sand extrusions onto a palaeo-seafloor are absent. Prior to drilling well 24/9-7 (2003), Volund was interpreted as a combination of depositional sandstone and sandstone intrusions from earlier exploration wells and seismic interpretation (Huuse *et al.* 2003). However, distinct fractured mudstones and brecciated facies in the cores from appraisal and development wells confirm the injected origin of all the reservoir sandstones when interpreted alongside the improved seismic image (De Boer *et al.* 2007; Townsley *et al.* 2012; Schwab *et al.* 2014; Hurst *et al.* 2016).

Near vertical exploration/appraisal wells 24/9-7, -7A, and -7B proved a 104 m thick oil column and a gas leg >150m and the commercial value of the Volund Field. The well data also allowed variations from the lower sill to the upper pinch out of the wing to be characterised.

Data

Multiple 3D seismic surveys are available over the Volund Field and reprocessing of these data is used to optimise the extraction of data from them. In this paper, the seismic volume shown was acquired in an NW-SW orientation in 1996 and reprocessed in 2014. A pseudo acoustic impedance (PAI) volume that is rotated 90 degrees so zero crossing is top sandstone with bulk shift of 10 m to fit the wells and forms the basis of this work. Volund sandstones are soft, i.e. low relative acoustic impedance compared to host rock mudstones. The resolution of the seismic allows sandstone units of 12-15 m thick to be resolved in the oil and water zones, this is improved to 3-5 m resolution when sandstones are gas filled. Top hydrocarbon-filled sandstones show larger-magnitude negative-amplitude values with offset on reflection seismic data and show as yellow and red on the figures. This means that the far-offset stack seismic volume is the best dataset on which to map/identify the top of the hydrocarbon-bearing interval and is shown in the figures. Changes in oil, gas and/or water concentrations due to production, are imaged on 4D seismic and add an additional source of data for mapping the reservoir.

Twenty wells penetrate the Volund reservoir that support confident calibration of the seismic interpretation. Cores from near vertical exploration and pilot wells allow interpretation of facies and

which can be link to wireline logs signatures. These interpretations can then be extrapolated into un-cored intervals using wireline logs, however, no image logs exist in the field. Six wells that intersect the southern wing are the focus of this study and their details summarised in Table 1. Gamma ray, density and neutron porosity borehole log data were used to derive porosity curves, these were calibrated with core data where available. Permeability curves were derived using porosity and also tied to core data (Townsley *et al.* 2012).

Reservoir architecture of the southern wing

The southern wing bounds the Volund Field to the south and is a large composite sandstone intrusion up to 250m high, dipping on average at 20-35° and with a surface area of least 5.7 km^2 (Fig. 2). Individual sandstone intrusions are up to 23 m thick (thickness perpendicular to bed dip in well 24/9-7 A). Horizontal development wells targeted the eastern side of the southern wing (Schwab *et al.*, 2014), and proved the sandstone intrusions to be laterally extensive (at least 900m) and sandstone rich (e.g. wells 24/9-P-2 AY1H and 24/9-P-10 BY1H). Well 24/9-P-10 BY3H was an exception with low net to gross (Fig. 3) but is similar to the earlier well 24/9-P-3 AH well to the north of the field (Fig. 1b).

A near horizontal sill (interpreted from core in wells 24/9-5 and 24/9-6, de Boer *et al.* 2007) occurs at the base of the wing (Fig. 2a) in which the sandstone heavy mineralogy is indicative of derivation from the adjacent underlying Hermod Sandstone (*pers. comm.* Elliot Foley and Andrew Morton, 2017). This is supported by production data where the Hermod aquifer provides pressure support to the intrusions for oil production (Townsley *et al.* 2012). Bifurcation and steps are present in the sill, similar to those known from outcrop (Hurst and Vigorito, 2017). The sill passes laterally into steeper units that form the low-angle to bedding intrusions of the wing (Fig. 2). Termination of the low-angle intrusions defines the top of wing, however in some places the wing changes into bed parallel upper sill that prograde away from the centre of the intrusion complex several kilometres. Part of the upper sill was cored in well 24/9-7B (Figs. 2c, 2d) and within the Volund Field this upper sill is entirely within the gas leg. The cause of the change from bed parallel sills to low angle intrusions and back into sills is not well documented but is likely affected by subtle heterogeneity changes in the host rock.

Seven boreholes penetrate Volund's south-eastern wing that, when combined with high quality 3D seismic data, give a unique opportunity to investigate the external and internal geometry of the intrusion. Within the wing, three sheet-like intrusions are mapped with confidence from 3D and 4D seismic ties to wells, and form a composite reservoir volume (Figs. 2d, 3). The intrusions, termed Front, Middle and Back, where Front is shallowest, are offset stacked and represented as discrete volumes in the 3D reservoir model (Fig. 4). The order of emplacement of the intrusions is not differentiated. The Front intrusion extends to shallower depth up to 250 m with 20-35° angle, and then becomes parallel to bedding continuing for several kilometres as an upper sill, with no evidence of extrusion onto a palaeo-seafloor. All three intrusions are in continuity with the lower sill, an interpretation that is consistent with production data (Townsley *et al.* 2012) and outcrop analogue data (Hurst *et al.* 2016; Scott *et al.* 2014; Grippa *et al.* 2019). This confirms a genetic link between deeper (sills) and shallower (wings) intrusions. Despite brightening and dimming in the oil zone on seismic data (Figs. 2a, 2c), which could indicate lithological heterogeneity, production data demonstrate good aquifer support and a high level of sandstone reservoir continuity between intrusions in the wing and the sill (Townsley *et al.* 2012). When modelled as a series of cross-sections calibrated by well data, Front, Middle and Back, thin and decrease in sandstone content upward (Figs. 4d, 4e, f, 5). Thinning of sandstone intrusions upward typically implies more tortuous connectivity between reservoir units

in an increasingly mudstone rich background. Mapping of individual intrusions within the wing is, to the best of our knowledge, an advance in the characterisation of the geometry of sub-surface sandstone intrusions and aligns with outcrop observations (Vigorito & Hurst 2010, Hurst & Vigorito 2017; Grippa *et al.* 2019).

Blocky, low gamma ray log profiles for sandstones with mudstone represented by higher gamma ray log profiles are characteristic of borehole logs throughout the sandstone intrusions in Volund (DeBoer *et al.* 2007; Schwab *et al.* 2014). From visual inspection of the core and grain size analysis, these sandstones show sparse indications of internal structures or variations in sorting (Fig 6a). Intervals with intermediate gamma- ray log profiles are present but difficult to interpret in the absence of core, which where available, reveals the presence of sand-supported mudstone clast breccia (Duranti & Hurst, 2004; Hurst *et al.* 2011). Mudstone clast breccia is common in Volund (Fig. 6; De Boer *et al.* 2007) and in outcrop (Kawakami & Kawamura, 2002; Hurst et al, 2003; Hurst & Vigorito, 2017; Zvirtes *et al*, this volume). Mudstone clasts in the breccia often have jigsaw clast geometry, micro-fractured clasts (sometimes sandstone filled, Figs. 6b, 6c), and irregular packing of predominantly angular mudstone clasts, including elongate filamentous (mm-thick) fragments. Some clasts have sharp curved contacts with the sandstone matrix. All these features are diagnostic of mudstone clast breccia derived from hydraulic fracturing and sand injection (Duranti & Hurst, 2004; Hurst *et al*, 2011).

Given the complexity of intrusions known from outcrop (Hurst *et al.* 2011; Hurst & Vigorito, 2017) it is not surprising that many, or most, small and steep (to bedding) sandstone intrusions present in the southern wing, are neither resolved nor detected by seismic data. Well penetrations however, reveal a complex bifurcation of sandstone within the seismic envelope in the shallow parts of the wing (Figs 2b, 5). Many of the thin sandstone units identified in wells show that upward bifurcation of intrusions forms progressively more thin intrusions, many of which are not resolved on the seismic data. Thin sandstone units (upper sills) in the Volund Field are only detected when gas-filled, in which case predominantly mudstone units with thin sandstone intrusions (N/G < 0.01) form "over" thickened reservoir intervals on seismic images (Fig. 2, well 24/9-7 B). General experience on Volund and in the neighbouring Viper-Kobra fields (Fig. 1; Skjærpe *et al.* 2018) demonstrates that penetration of thin sandstones is typical in the shallow sections of wings. As the thin parts of wings connect to thicker, down-dip reservoir units, they are important for optimising recovery by placing well completion in shallower but, low N/G intervals. The benefits are placement of production intervals to target attic oil, which are higher above the aquifer and delay water breakthrough. Consideration to the expansion of the gas cap is also evaluated from interpretation of the 4D seismic and in some places post production pilot wells before targeting this attic oil.

Distribution of wells in the Front, Middle and Back intrusions (Figs 1b, 3a) allows investigation of variations in reservoir porosity with increasing distance from the feeder sill and depositional parent units (Hermod Sandstones) and also along strike. Data from vertical and near vertical wells exemplify depth related variations (Fig. 7), and horizontal wells exemplify the along-strike relationships (Fig. 9).

Intruded sandstones are the only reservoir units present in the Volund Field. They form sections of clean injected sandstones (colour coded yellow) or are intermixed with fractured mudstones forming the brecciated facies (colour coded green). Non reservoir facies are mudstones and forms the host rock into which the sands are intruded (colour coded white). Facies are defined from cored sections, their characteristic log signatures from well logs identified, and interpreted in uncored sections based primarily on gamma ray, neutron, density, resistivity and interpreted porosity logs. There are three

distinct classes of porosity, high related to intruded clean sandstone facies, low related to the host rock mudstones and mid values related to the brecciated facies.

Depth related variation in porosity

Porosity in the Front intrusion in well 24/9-7 has generally high values, close to the Volund Field average of 34% (Fig 7a & b). Where lower porosity (close to 20%) is encountered, this is associated with thin sandstone units and mudstone clast breccia (Fig. 7a). Lack of resolution of borehole logs, and the "edge effects" on logs that prevail when thinly bedded strata are encountered, create an intermediate artefact porosity and fail to differentiate between mudstone and sandstone. A deeper, 45 m thicker section of the Front intrusion in well 24/9-7A is sand-rich and has uniformly high porosity of 35% (Fig. 7b). There is no observed depth trend with porosity in the Front intrusion (Fig. 8). Deeper, and offset to the east (Fig. 3a), well 24/9-7A penetrates the Back intrusion (Fig. 7c) in which porosity is very similar to the shallower Front intrusion ranging between 34-36% (Fig. 7b, 8). For comparison, the deeper lower sill that feeds the wings has a porosity of 35-37%.

Strike related variation in porosity (from horizontal wells)

Horizontal wells drilled along strike of the Front intrusion typically have uniformly high porosity, for example, well 24/9-P-10 BY1H (Fig. 9a). Intervals with approximately zero porosity are mudstone, encountered when the borehole exited the top or base of the intrusion when drilling along strike. Where intermediate porosity is computed, we infer the presence of mudstone clast breccia (Fig. 9a & b). Although core and image logs are unavailable in the horizontal wells, comparison of data from wells where core data are available, shows that reservoir facies with <30% porosity are typically breccia facies that are preserved along the margin of sandstone intrusions with mudstone clasts from the hydraulically fractured host mudstone mixed into the sandstone intrusions.

In the thick section of sandstone in the Middle intrusion (Fig. 10), where it is comparable to the sandstone intrusion in the Front intrusion (Figs. 9a, 9b), porosity is similarly high and uniform (average porosity of 35%). At the right side of the plot, from approximately 130 m onward, well data suggests the well exits the intrusion into host mudstone then re-enters the intrusion through a brecciated interval.

In the Back intrusion, horizontal well 24/9-P-10 BY3H has markedly different porosity (Fig. 11) with average porosity of 24% compared to the Volund Field average of 34%. The near vertical well 24/9-7A encountered the Back intrusion and the sandstone penetrated had porosity of 35%, similar to the field average and the Front intrusion (Fig. 7c). Although some high porosity (>30%) sections occur in the horizontal well, the generally less porous sections are the combined effect of the borehole exiting and re-entering the Back intrusion along strike and encountering mudstone clast breccia as addition to host mudstone (Fig. 11). The consequence is borehole logs measure the combined effects of sandstone and mudstone that lowers the porosity estimates. Well 24/9-P-10 BY3H penetrated shallower in the Back intrusion than near-vertical well 24/9-7A, and the higher mudstone (lower computed porosity) in the former well is consistent with more mudstone-rich facies in shallower parts of wings.

Wing: analysis of porosity distribution

As a single entity, sandstone in the southern wing has a skewed normal distribution with most data lying in the 32 to 38% range (Fig. 12). Comparison of porosity data from the Front and Middle intrusions reveals very similar trends (Figs. 13a, 13b). Porosity distribution in the Back intrusion is very different, with most data between 16 and 23%, and a small cluster of data between 33 and 37%

(Fig. 13c). Display of data from near vertical well 24/9-7B (Fig. 13d) has a similar distribution to data from the Front and Middle intrusions (Figs. 13a, 13b), which highlights the contrast in lithology sampled in well 24/9-P-10 BY3H where breccia is inferred to be a significant component of the reservoir section. In Fig. 13c, fifteen of the twenty-three data points in the 34-37% porosity range come from well 24/9-7B. Excluding porosity data from the mudstone clast breccia in well 24/9-P-10 BY3H, the three sandstone intrusions that comprise the southern wing have uniformly high porosity (largely 33-35%) with respect to depth and along strike.

Plotting porosity data from all wells in the Front intrusion against vertical distance from the point of contact with the sill, there are two trends: 1) throughout the section, high porosity (30 to 38%) sandstone is present; 2) above 100m from the sill more than half the data have porosity of 25% or less (Fig. 14). As described earlier, trend 1 demonstrates the presence of high porosity sandstone independent of depth. Trend 2 is more complex and depicts the facies variation from relative thick intervals of clean sandstone to a thinner units of sandstones interfingering with higher concentration of mudstone clast breccia (well 24/9-7, Fig. 7a) as increased bifurcation of the intrusion upward from the sill (Figs. 2, 5).

Core permeability distributions from core have been presented by Townsley *et al.* 2012. Relationship between core porosity versus core permeability from wells 24/9-7 and 24/9-7A are illustrated in Fig. 15. As described the porosity in the sandstones are clustered close to the mean of 34%. The corresponding permeabilities values are more varied but cluster between 1 and 8 Darcy. Lower permeability values occur when the porosity is less than 30% and link to the presence of breccia facies.

Discussion

Outcrop of sandstone wings and saucer-shaped intrusions demonstrates that they are composites of connected, smaller intrusions (Hurst *et al.* 2011; Grippa *et al.* 2019). Thus, identification of composite intrusions in subsurface injection complexes such as the Volund southern wing is not surprising but historically been difficult due to seismic resolution limitations. To the best of our knowledge, this is the first documentation of the composite internal structure of a subsurface wing intrusion.

Resolving wing geometry

Since positive identification of wing geometry along the margin of Alba field (MacLeod *et al.* 1999; Duranti *et al.* 2002), wings have become important targets for development drilling, and latterly as exploration targets. Volund's southern wing was the first sandstone intrusion targeted by an exploration well (De Boer *et al.* 2007) and was the focus for the initial development wells (Townsley *et al.* 2012; Schwab *et al.* 2014). One cannot map what is unseen, and interpretation of seismic data is no exception to this, however by integrating knowledge of reservoir-scale outcrop analogues into subsurface interpretation, identification of cogent features is better informed. Knowing from outcrop that wings are typically internally heterogeneous was a significant driver in seismic interpretation of the southern wing. Complementary to the geological understanding of the internal complexity of the southern wing (Figs 2, 3,4, 5), is the evolution of seismic data quality, which is illustrated by comparison data in De Boer *et al.* (2007), Schwab *et al.* (2014) and this study.

Although the volume between top and base of the southern wing is well defined (Fig. 2), there is little evidence of the intricacy caused by upward bifurcation and thinning of intrusions exemplified by borehole data. Increased significance of mudstone upward in the wing is evidenced by borehole (logs) data (Figs 7a & 9) the precise character of which is confirmed when core contains mudstone clast

breccia or mudstone units (Fig. 6). When considered collectively, borehole data show that the occurrence of more mudstone clast breccia upward and specifically when approximately >100m from the sill (Fig. 14), is a systematic trend in each of the three sandstone intrusions. The cause of the stepping and bifurcation of the intrusions is most likely linked to small heterogeneities in the host mudstones caused by grain-size and mineralogy changes and the resulting development of fractures. Unlike many depositional reservoirs in which reservoir quality and connectivity decrease as interbedding with mudstone increases, in the southern wing reservoir quality remains good with excellent vertical and horizontal connectivity (Towsley *et al.* 2012; Schwab *et al.* 2014).

Porosity

Uniformly high porosity (about 35%) is characteristic of the sandstone intrusions. Lower average porosity is associated with the presence of mudstone, either as larger proportions of thicker host strata up-dip along the intrusions i.e. thinner sandstone intrusions (Figs 2d, 4, 5) or as mudstone clasts within a sandstone intrusion matrix forming mudstone breccia (Fig. 6). Further detailed consideration of mudstone clasts is in the following section. There is no evidence of significant silica or silicate diagenesis in the Volund reservoir and the clay-sized particles present in pores are of detrital origin (Fig. 3 in Hurst *et al. this volume*). Absence of a relationship between average porosity and depth (Fig. 8) is largely a function of the lack of silica and silicate diagenesis that are thermally driven cements. Pore-occluding calcite cement is occasionally present and constitutes a drilling hazard in otherwise poorly consolidated strata but is volumetrically insignificant. Pyrite is significantly subordinate to calcite and when abundant (maximum <5%) skews the formation density log toward lower than actual porosity. For comparison, in the Volund exploration wells, porosity in the deeper Hermod sandstone are 28% on average (Townsley et. al 2012), the parent unit and source of sand to the Volund intrusion. This is significantly lower than the porosity in the intruded sill and the wings (Fig. 14) and implies some improvement in porosity due to the remobilisation and intrusion of the sands.

Mudstone clast breccia

Mudstone clast breccia (*sensu* Duranti & Hurst 2004), is diagnostic of sandstone intrusions, and is derived from collapse of intensely hydraulically fractured host strata into dilated fractures during sand injection (SIRG, *unpublished data*). Significant underestimation of reserves is a frequent characteristic of intrusive traps and their constituent sandstone intrusion reservoirs, historically on the Volund Field this can be up to 30% (Satur et.al. 2017). An important component of the underestimation is that many thin and steep sandstone intrusions are neither resolved nor detected on well logs (Grippa *et al.* 2019). A further component is that mudstone clast breccia is a reservoir facies that is often difficult to differentiate from non-pay mudstone-dominated units unless core is available (Fig. 6). Sometimes, 10's m thick units of mudstone clast breccia develop more regionally (Zvirtes *et al. this volume*). Many sandstone intrusions have approximately binary lithogical systems, fine- to medium-grained sandstone and mudstone, which lack intermediate grain size gradation. Mudstone clast breccia is similarly binary with the main variable the concentration and size of mudstone clasts; texturally the angularity of mudstone clasts may vary (Duranti & Hurst 2004; Hurst & Vigorito 2017).

Average porosity derived from borehole log analysis in the Back intrusion of Volund's southern wing is 24% compared to the Volund Field average of 34% (Figs. 9, 13b, 13c). In depositional systems, a similar reduction in borehole-log derived average porosity is typically associated with reduction in average grain size, poorer sorting, higher clay/mudstone content and surface area to volume ratio. When hydrocarbon saturated, higher irreducible water saturation and lower permeability are all

indicative of reduced reservoir quality. This type of relationship is unlikely in the binary lithological system of sandstone intrusions and demonstrated by the sandstone encountered in well 24/9-7A (Fig. 7a). Good quality reservoir sandstone is known to co-exist with clasts of mudstone when core enables observation and measurement of reservoir quality (Fig. 6); in mudstone clast breccia the storage capacity per unit volume of reservoir decreases but reservoir quality, specifically permeability, remains similar to that in adjacent sandstone intrusions without mudstone clasts (Fig. 6; De Boer *et al.* 2007). The porosity is so consistent in the sandstone that estimation of sandstone to mudstone proportions in the breccia is possible using the computed porosity values, which represent the weighted average of the sandstone and mudstone.

Mudstone clast breccia, and a generally increased content of mudstone clasts, are associated with the margins of sandstone intrusions, and the latter often degrade reservoir quality (Scott *et al.* 2009; Scott *et al.* 2013). Well 24/9-P-10 BY3H (Back intrusion) penetrated a sandstone-poor section (low N/G of 19% including breccia facies with on average 50:50 ratio of sandstone to mudstone) in which mudstone clast breccia and host mudstone strata are common (Figs. 13c, 13d). Despite the low N/G the well is productive, from which it is inferred that the main contribution to the low N/G is mudstone clast breccia and host mudstones rather than finely comminuted clay grains, which would exert a strong influence on reservoir quality (Scott *et al.* 2013). This interpretation is similar in character to another well in the northern wing (well P3, Fig 1), in which low N/G (24%) prevails and has recorded good production rates through connectivity downward to large volumes of high N/G sandstone and ultimately, the aquifer (Townsley *et al.* 2012; Schwab *et al.* 2014, Satur *et al.* 2017).

Conclusion

Well and seismic data on the Volund Field allows mapping and characterisation of an injection wing. The numerous near vertical and horizontal wells that have penetrated the southern wing of the Volund injection complex, and good quality of the seismic data, allows detailed characterisation of the intrusions. Key observations include:

1. The southern wing on the Volund Field comprises three seismic scale sandstone intrusions (Front, Middle and Back). This form stacked units with some degree of lateral offset. The Front intrusion extends shallower than the Middle and Back intrusions and continues for several kilometres as a sill with no evidence of extrusion onto a palaeo-seafloor.
2. Seismic mapping on 3D and 4D datasets, pressures in wells and production history show that the intrusions connect at depth to the same feeder sill complex and aquifer. Outcrop analogues support this observation, which is suggestive that a sub-seismic intrusion network connects the intrusions.
3. The Front intrusion is composed of high porosity sandstone that varies very little in the strike section (as demonstrated by horizontal wells) or with depth (as demonstrated by near vertical wells). There are weak trends in porosity variation within the wing until 100m vertical distance from the feeder sill where bifurcation and mudstone breccia may be the cause of a greater spread in porosity values. Porosity values in the southern wing are lower than their inferred parent units in the Hermod Sandstone but similar to the feeder sill.
4. All three intrusions have similar sandstone porosity, which are high and show very little variation. One well (24/9-P-10 BY3H) is an exception, where lower porosity is attributed to

the wellbore exiting and re-entering the intrusion along strike on multiple occasions with only short intervals of sandstone penetrated.

5. Intervals in wells interpreted to have porosity lower than approximately 30%, and where sandstone appears to be hetrolithic or shaley, inference is made of the presence of a mudstone clast breccia. Breccia is easily recognised in core but less obvious on borehole logs. Reservoir characteristics of breccia may be unrecognised from analysis of borehole logs, but in the Volund Field contributes significantly to reservoir volume and connectivity. Interpretation of breccia as non-reservoir leads to significant reserve underestimation, and during drilling could adversely affect geosteering decisions.

Acknowledgements:

Aker BP ASA and licence partners Lundin Norway AS are thanked for permission to publish. The authors wish to thank previous development and production geoscientist and engineers who have contributed to the current understanding of the Volund Field. Aker BP acknowledge the Sand Injection Research Group, for their contribution to knowledge and understanding. Comments from two anonymous reviewers were valuable.

References

De Boer, W., Rawlinson, P.B. & Hurst, A. 2007. Successful exploration of a sand injectite complex: Hamsun Prospect, Norway Block 24/9. *In*: Hurst, A. & Cartwright, J. (eds) Sand Injectites: Implications for Hydrocarbon Exploration and Production. American Association of Petroleum Geologists, Tulsa, OK, Memoir, **87**, 65–68.

Duranti, D. 2007. Large-scale sand injection in the Paleogene of the North Sea: modelling of energy and flow velocities. *In*: Hurst, A. & Cartwright, J. (eds) Sand Injectites: Implications for Hydrocarbon Exploration and Production. American Association of Petroleum Geologists, Tulsa, OK, Memoir, **87**, 127–138.

Duranti, D. & Hurst, A. 2004. Fluidisation and injection in the deep-water sandstones of the Eocene Alba Formation (UK North Sea). Sedimentology, **51**, 503–531.

Duranti, D., Hurst, A., Bell, C. & Groves, S. 2002. Injected and remobilised sands of the Alba Field (UKCS): sedimentary facies characteristics and wireline log responses. Petroleum Geoscience, **8**, 99–107.

Foley, E. 2017. Constraining the provenance of the Volund, Viper and Kobra sand injectite complexes of the Norwegian North Sea, using heavy mineralogy. Unpublished MSc thesis, University of Aberdeen, 218.

Hurst, A., Cartwright, J.A., Huuse, M., Jonk, R., Schwab, D., Duranti, D. & Cronin, B. 2003a. Significance of large-scale sand injectites as long-term fluid conduits: evidence from seismic data. Geofluids, **3**, 263–274.

Hurst, A., Cartwright, J.A. & Duranti, D. 2003b. Fluidisation structures in sandstone produced by upward injection through a sealing lithology. *In*: van Rensbergen, P., Hillis, R.R., Maltman, A.J. & Morley, C.K. (eds) Subsurface Sediment Mobilization. Geological Society, London, Special Publications, **216**, 123–137.

Hurst, A., Cartwright, J.A., Duranti, D., Huuse, M. & Nelson, M. 2005. Sand injectites: an emerging global play in deep-water clastic environments. *In*: Dore´, A. & Vining, B. (eds) Petroleum Geology: North-West Europe and Global Perspectives. Proceedings of the 6th Petroleum Geology Conference. Geological Society, London, 133–144.

Hurst, A., Scott, A. & Vigorito, M. 2011. Physical characteristics of sand injectites. Earth-Science Reviews, **106**, 215–246.

Hurst, A., Huuse, M., Duranti, D., Vigorito, M., Schwab, A.M. & Jameson, E.W. 2016. Application of outcrop analogues in successful exploration of a sand injection complex, Volund Field, Norwegian North Sea. *In*: Bowman, M., Smyth, H.R., Good, T.R., Passey, S.R., Hirst, J.P.P. & Jordan, C.J. (eds) 2016. The Value of Outcrop Studies in Reducing Subsurface Uncertainty and Risk in Hydrocarbon Exploration and Production. Geological Society, London, Special Publications, **436**, 75–92.

Hurst, A. and M. Vigorito, 2017, Saucer-shaped sandstone intrusions: An underplayed reservoir target: AAPG Bulletin, **101**, no. 4, p. 625–633.

Huuse, M., Duranti, D., Cartwright, J.A., Hurst, A. & Cronin, B. 2001. Seismic expression of large-scale sand remobilisation and injection in Paleogene reservoirs of the North Sea Basin and beyond. *In*: 63rd EAGE Conference and Technical Exhibition. Amsterdam, 2001, Paper **L-07**.

Huuse, M., Duranti, D. *et al.* 2002. Detection, origin and significance of large-scale injected sand bodies in the North Sea Cenozoic. *In*: 64th EAGE Conference & Technical Exhibition. Florence, 2002, Paper **H-19**.

Huuse, M., Duranti, D. *et al.* 2003. Sandstone intrusions: detection and significance for exploration and production. First Break, **21**, 33–42.

Huuse, M., Cartwright, J.A., Gras, R. & Hurst, A. 2005. Km-scale sandstone intrusions in the Eocene of the Outer Moray Firth (UK North Sea): migration paths, reservoirs, and potential drilling hazards. *In*: Dore´, A. G. & Vining, B. (eds) Petroleum Geology of NW Europe: Proceedings of the 6th Conference. Geological Society, London, 1577–1594.

Huuse, M., Cartwright, J.A., Hurst, A. & Steinsland, N. 2007. Seismic characterization of large-scale sandstone intrusions. *In*: Hurst, A. & Cartwright, J.A. (eds) Sand Injectites: Implications for Hydrocarbon Exploration and Production. American Association of Petroleum Geologists, Tulsa, OK, Memoirs, **87**, 21–35.

Macleod, M. K., Hanson, R. A., Bell, C. R. & McHugo, S. 1999. The Alba field ocean bottom cable seismic survey: impact on development. The Leading Edge, **18**, 1306–1312.

Townsley, A., Schwab, A.M. & Jameson, E.W. 2012. The Volund Field: Developing a unique sand injection complex in Offshore Norway. Paper **SPE 154912**, presented at the Europec Conference, Copenhagen, June.

Satur, N., Bang, A., Skjærpe I. & Muehlboeck, S. 2017. Applying lessons learnt from the Volund Field to understand the injectite play. Presented at Hydrocarbon Habitats Conference, Oslo, Norway Feb 2017.

Schwab, A.M., Jameson, E.W. & Townsley, A. 2014. Volund Field: development of an Eocene sandstone injection complex, offshore Norway. *In*: MacKie, T. (ed.) Geological Society, London, Special Publications. http://doi.org/10.1144/SP403.4

Scott, A.S.J., Vigorito, M. & Hurst, A. 2009. The process of sand injection: internal structures and relationships with host strata (Yellowbank Creek Injectite Complex, California, U.S.A.). Journal of Sedimentary Research, **79**, 1–18.

Scott, A., Hurst, A. & Vigorito, M. 2014. Outcrop-based reservoir characterization of a kilometre scale sand injectite complex. AAPG Bulletin, **97**, 309–343

Szarawarska, E., Huuse, M., Hurst, A., De Boer, W., Lu, L., Molyneux, S. & Rawlinson, P.B. 2010. Three-dimensional seismic characterisation of large-scale sandstone intrusions in the lower Palaeogene of the North Sea: completely injected v. in situ remobilised sandbodies. Basin Studies, **22**, 517–532.

Vigorito, M. & Hurst, A. 2010. Regional sand injectite architecture as a record of pore pressure evolution and sand redistribution in the shallow crust: insights from the Panoche Giant Injection Complex, California. Journal of the Geological Society, **167**, 889–904.

Vigorito, M., Hurst, A., Cartwright, J.A. & Scott, A. 2008. Regional-scale subsurface sand remobilization: geometry and architecture. Journal of the Geological Society, **165**, 609–612.

Table 1. Table summarising the wells that penetrate the eastern portion of southern wing of the Volund Field, the focus of this study.

Well Name	Well Type	Average Well Deviation* in reservoir section	Year Drilled
24/9-6	Exploration	1	1994
24/9-7	Exploration	2	2004
24/9-7A	Appraisal	30	2004
24/9-7B	Appraisal	29	2004
24/9-P-2H	Geo-Pilot	67	2009-10
24/9-P-2-AY1H	Production	90	2010
24/9-P-10H	Geo-Pilot	42	2016
24/9-P-10-BY1H	Production	90	2017
24/9-P-10-BY3H	Production	90	2017

* well deviation of 0° is vertical, 90° is horizontal

Figure Captions

Fig.1: (**a**) Location map of the Volund Field in the Norwegian North Sea. (**b**) Volund Field top reservoir and top injection complex depth map in meters. Many wells penetrate the 20-35°dipping wings, with long horizontal oil production wells following the strike of the dykes. The exploration and appraisal wells on the field are labelled along with some production wells discussed in this study.

Fig.2: (**a**) Far-stack, a relative acoustic impedance seismic depth section and geo-seismic interpretation of the Volund injection complex showing the sill and injection wing composed of multiple intrusions. Yellow rectangles alone the well path indicated presence of sandstone in the wellbore. The underlying depositional Hermod Sandstone is the source of sand, and the Heimdal is thought to be the source of the water budget that allowed the injectite to form. Heimdal contributing with water to facilitate injection. The black dashed line marks the Top Balder Fm. which shows a clear offset or jack-up associate with the intruded sandstones. Gas-Oil Contact (GOC) and Oil-Water Contact (OWC) indicated, vertical exaggeration x2. (**b**) Seismic depth section and geo-seismic section with focus around on the 2004 appraisal wells that proved the injection concept on Volund Field and a 104m thick oil column. Interpretation of intruded sandstones showing a bifurcation pattern of sandstones beds with shallowing depths. The Front and Back intrusions are visible in this section (Middle intrusion is located off this line of section). Note the strong seismic amplitudes in thin gas filled sandstones beds in 24/9-7B well that over-represent the sandstone thickness observed in the well. Dashed orange lines are conceptual injected sandstones with indications from disturbed seismic and on outcrop observations. Location of cored intervals are highlighted in magenta.

Fig.3: Depth map of the base of the Volund Injection complex (2x vertical exaggeration) with focus in an area of the southern wing of the field (see Figs. 1, 2). Exploration and appraisal wells from 2004 in black (24/9-7, -7A, -7B), 2016 pilot well in grey (24/9-P-10H) and production wells in blue (24/9-P-2 AY1H, -P-10 BY1H, -P-10 BY3H). Sandstone and mudstone flags as penetrated in the wells are shown in the well bores, note breccia facies are generally included in the mudstone flag. High net to gross is observed in the intrusions. The exception is well 24/9-P-10 BY3H, which has significant lower net sand along the wellbore.

Fig.4: Interpreted lateral extent of the (**a**) Front, (**b**) Middle and (**c**) Back intrusion as interpreted from seismic (3D and 4D) and well penetrations and modelled in a 3D reservoir model grid. Underlying depth surface is base of the Volund injection complex (20m contour spacing, 2x vertical exaggeration). The intrusions display lateral offset staking and vary in the depth they protrude upward. The Back and intrusions appear to terminate at similar depths however the Front intrusion reach shallower depth before extending parallel to strata and thus changing into an injected “sill”. However, 4D seismic and production data suggests they are connected to the left (north) of the image into a “feeder” sill. (**d**) Sections through the 3D reservoir model showing the Front, Middle and Back intrusion illustrating the vertical relationship between them. (**e**) Entire complex and (f) selected cross sections showing sandstone and mudstone/breccia within the intrusions (note host rock mudstones between the dykes not visualised) show decrease in sand with shallower depth. Entire grid of the injected sandstone and mudstones within the injection wing.

Fig.5: Reservoir model from the Front intrusion, (**a**) sections through the 3D grid and (**b**) the entire grid showing sandstones and mudstones that are part of the injected dyke. The model reflects an updip increase in mudstone content, bifurcation and thinning of the sandstone beds within the Front intrusion and it transitions into bed parallel “sill that can be mapped to extend several km beyond the image. Due to the vertical grid resolution, these thin sands are not resolved in the facies model. The apparent break in continuity of the intrusion (white oval) is not apparently real and most likely reflects a reduction in seismic imaging due to near vertical step in the intrusions. Underlying depth surface is the base of the Volund injection complex.

Fig.6: Core photos (**a**) Homogeneous injected sandstones, the primary reservoir facies in the Volund Field. (**b**) Irregular sided injected sandstones penetrate through host rock mudstones forming jig-saw shaped mudstone clasts as they are hydraulically fractured and later the fractures filled with sand. (**c**) Injection sandstone with upper erosive surface and mudstone clasts being incorporated into the injected sandstones. Also hydraulically

fractured mudstone with some fractures filled with sand (arrow). (**d**) Injected sandstones with associated mudstone injection breccia, with injection occurring in multiple phases. Photos b, c and d would be classified as breccia facies from well logs. In all photos, the core is 9 cm wide.

Fig.7: Computed porosity logs, tied to core porosity where available, along the near vertical wells in the southern wing with facies interpretation. Distance is along the well bore in meters. (**a**) Well 24/9-7 intersect the Front intrusion in an up-dip location and display more hetrolithic facies and varied porosity. However, where the sand units are not thin, the porosity is close to the average for the front intrusion. (**b**) Well 24/9-7A intersect the centre of the intrusion with a uniform porosity in the sand facies, close to the average. (c) Porosity and facies interpretation of the Back intrusion with again uniform and high porosity in the sand facies. Within the sand facies, the porosity is high and uniform, lower porosity values are encountered in breccia and host rock mudstones.

Fig. 8: Sandstone porosity plotted with depth for the Front and Back intrusion from the near vertical wells, and an average value for the middle intrusion where the usable data is from a horizontal well. There is no clear depth trend in porosity and intrusions have predominantly similar sandstone porosity of 30-37%.

Fig.9: Porosity log and facies for the two horizontal production wells in the Front intrusion that are drilled along strike of the intrusion. (**a**) Well 24/9-P10 BY1H penetrates a 650 m strike section with sandstones with uniformly high porosity are occasionally interrupted by mudstones as the well exits the intrusion. Breccia facies with intermediate porosity are observed of the well exemplified by the zoomed in section (**b**). (**c**) A similar observation is identified in another horizontal well 24/9-P10 AY1H in the Front intrusion and in (**d**) well 24/9-P10 BY3H for the Middle Intrusion.

Fig. 10: Porosity log and facies for the Middle intrusion. Horizontal well 24/9-P10 BY3H has uniform porosity averaging 34% in the sandstone facies. The low net sand fraction reflects the thin nature of the reservoir with the wellbore exiting and re-entering the reservoir along strike. Despite this, all the sandstone penetrated have high resistivity values showing presence of oil and some degree of connectivity to allow oil migration. Some sections of the well where the density and neutron logs indicate mudstone also have high resistivity values and oil present, these are interpreted as breccia facies.

Fig.11: Porosity log and facies for the Back intrusion. Horizontal well 24/9-P10 BY3H that has high variability in sand penetration, thickness and porosities along its length. The reason for this variability is attributed to the wellbore exiting and re-entering the strike of the intrusion along the wellbore. Intervals of low gamma ray log (e.g. 55m) with clear sand indicate clean injected sandstones. Interval 475-550m with higher gamma ray log, poorer sand indication but hydrocarbon bearing as indicated from high resistivity is typical of breccia facies. The breccia in this interval could be identified from the density and neutron logs, however more difficult to interpret in other section (e.g. 250-300m).

Fig.12: Frequency distribution plot of 3,650 log porosity values from 25 wells on the Volund Field. Porosities come from the computed porosity logs that are tied to core porosity where available. The data is extracted from the interpreted sandstone facies only, showing porosities between 30-38% most common. Lower porosities are associated with breccia facies or log edge effects at sandstone - mudstones boundaries.

Fig.13: Distribution of sand facies porosity values in the wells penetrating the eastern part of the southern wing, porosity logs sampled every 1m along the wellbore. The Front (**a**) and Middle (**b**) intrusions show a similar distribution with predominant porosities of 34%. The few data points in the figures that show low porosities reflect cemented sandstones. (**c)** The Back intrusion is different and show lower porosities and a larger spread (due to log edge effects due to the varied facies changes) but when data from only the vertical wells is used (**d**), there is a similar pattern to the Front and Middle intrusions is observed.

Fig. 14: The Front injected dyke porosity values in sand facies plotted against vertical distance from the down-dip “feeder” sill. Up to 100 m from the sill, the porosity values show little spread and uniformly between 32-37%. The average porosities from the two 1993-4 exploration wells (24/9-5 and -6) penetrating the sill are

plotted with triangles and have values of 35-36%. At greater distance the spread in porosity increases, a reflection of bifurcation of the intrusions, thinner sandstone beds and well logs being affected by edge effects due facies changes (e.g. more variable values shown in well 24/9-7, see Fig. 9). Note for the horizontal wells, the average sand porosity every 100m is used so these data points are not over represented.

Fig. 15: Permeability-porosity plot of data extracted from cores in wells 24/9-7 and 27/4-7B where there is a bias to sample the sandstones facies. The average permeability and porosity values are highlighted. The data shows there is a cluster of data in a relatively small range of porosities and permeabilities. Some of the lower values could be sandstones where there is a degree of mud clasts, often linked to breccia facies.

Fig 1

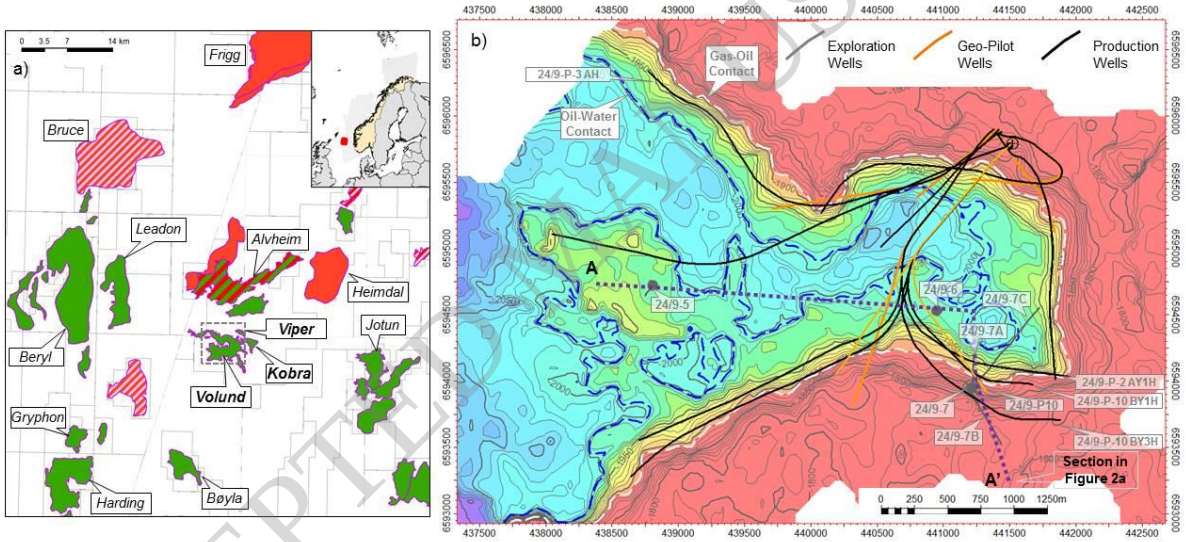

■ Fig 2 a